

High Dielectric Constants of Composites of Fiber-Like Copper Phthalocyanine-Coated Graphene Oxide Embedded in Poly(arylene Ether Nitriles)

JINGWEI LI,¹ ZEJUN PU,¹ ZICHENG WANG,¹ YA LONG,¹ KUN JIA,^{1,2}
and XIAOBO LIU^{1,3}

1.—Research Branch of Advanced Functional Materials, Institute of Microelectronic and Solid State Electronic, High-Temperature Resistant Polymers and Composites Key Laboratory of Sichuan Province, University of Electronic Science and Technology of China, Chengdu 610054, People's Republic of China. 2.—e-mail: jiakun@uestc.edu.cn. 3.—e-mail: liuxb@uestc.edu.cn

The surfaces of graphene oxide (GO) sheets were coated with fiber-like copper phthalocyanine (CuPc) by use of a solvothermal process. The product, GO@CuPc, was used as a filler in high-performance poly(arylene ether nitrile) (PEN) composites. Films of the composites had high thermal stability, and glass-transition temperatures in the range 170–182°C. Thermogravimetric analysis revealed their initial decomposition temperatures were in the range 470–483°C. Scanning electron microscopy showed that dispersion of GO@CuPc in PEN was much better than that of unmodified GO; this can be attributed to relatively strong interaction between GO@CuPc and the PEN matrix. All the composite films were highly flexible and had enhanced mechanical properties. Tensile strengths of the composites were as high as 89 MPa in the presence of 1 wt.% GO@CuPc, an increase of 20% compared with pure PEN film. Dielectric constants of the composite films were as high as 52 at 100 Hz when the GO@CuPc content was 5%. Because of these excellent mechanical and dielectric properties, PEN/GO@CuPc composites have much potential for use as film capacitors.

Key words: Poly(arylene ether nitriles), copper phthalocyanine, graphene oxide, composites, mechanical properties, dielectric properties

INTRODUCTION

As engineering thermoplastic resins, poly(arylene ether nitriles) (PEN) have attracted much industrial and academic interest, because of their outstanding properties, which are similar to those of polyether ether ketone (PEEK).¹ Because of their rigid molecular structure, PEN have excellent thermal stability, radiation resistance, and molding workability;^{2,3} they can, thus, be used at high temperature in harsh chemical environments. However, the low dielectric constants (ca. 3–4) of PEN hinder their application in advanced electronics.

Recently, graphene nanosheets (GNs) have been recognized as potential nanosized fillers, because of such unique properties as outstanding thermal stability, excellent in-plane electrical conductivity, and large surface area-to-mass ratio.^{4,5} However, pure graphene accumulates and restacks naturally, because of its high cohesive energy and strong p–p stacking tendency, resulting in inhomogeneous dispersion in the polymer matrix. Surface modification of graphene is, thus, indispensable for enhancing its dispersion within the polymer matrix and optimizing the performance of the resulting composite materials.

Graphene oxide (GO) has attracted much attention in many disciplines, for example the electronics industry, bio-medicine, and catalysis.^{6–11} However, bare GO has poor interface compatibility with PEN

(Received November 5, 2014; accepted February 12, 2015; published online March 6, 2015)

polymers, because of the presence of such oxygen-containing functional groups as hydroxyl, epoxy, carbonyl, and carboxyl.^{12,13} CuPc (copper phthalocyanine), an organic dielectric material with intrinsic electric conductivity and a high dielectric constant, is expected to improve the compatibility between GO and PEN as medium.¹⁴ Because of the similar structures of CuPc and PEN, the GO@CuPc could be well distributed in the PEN matrix, leading to significant enhancement of the dielectric, mechanical, and thermal properties of the composites.

In this study, to improve the mechanical and dielectric properties of PEN composites, the PEN/GO@CuPc composite films with different GO@CuPc content were fabricated by use of a solution-casting method. The films were investigated systematically by use of Fourier-transform infrared spectroscopy (FTIR), ultraviolet–visible (UV–vis) absorption spectroscopy, scanning electron microscopy (SEM), and transmission electron microscopy (TEM). The thermal, mechanical, dielectric, and rheological properties of the composite films were also investigated systematically.

EXPERIMENTAL

Materials

Poly(arylene ether nitriles) were synthesized by nucleophilic aromatic substitution polymerization of the monomers 2,6-dichlorobenzonitrile (DCBN) and bisphenol A (BPA), in *N*-methyl-2-pyrrolidone (NMP), with anhydrous K_2CO_3 as catalyst. NMP was supplied by Tianjin Bodi chemicals (Tianjin, China). 4-Nitrophthalonitrile (99%) was purchased from Alpha Chemicals (Dezhou, China). 4,4'-bis(3,4-Dicyanophenoxy)biphenyl (BPh) was synthesized in our laboratory.¹⁵ Graphene oxide was prepared by means of the modified Hummers method.¹⁶ All chemicals and reagents were used without further purification.

Preparation of GO@CuPc Hybrids

For synthesis of fiber-like GO@CuPc hybrids, GO (0.1 g), 4-nitrophthalonitrile (1.35 mmol), BPh (0.45 mmol), and copper acetate dihydrate ($Cu(OAc)_2 \cdot 2H_2O$) (0.20 mmol) were added sequentially to 40 mL ethylene glycol (EG). The mixture was stirred vigorously for 30 min, by use of a mechanical stirrer, then sealed in a Teflon-lined stainless-steel autoclave. The autoclave was maintained at 160°C for 15 h with ethylene glycol up to 80% of the total volume, then left to cool naturally to room temperature. The products were washed with distilled water and acetone, separately, to remove residual BPh, then dried at 50°C for 8 h.

Preparation of PEN/GO@CuPc Composite Films

PEN/GO@CuPc composite films were fabricated on a glass plate by use of the solution-casting

method combined with ultrasonic dispersion. To ensure the GO@CuPc hybrids were uniformly dispersed in the polymer matrix, they were dispersed in NMP by use of violent ultrasonic treatment. To prepare PEN solution, purified PEN was dissolved in NMP by heating and mechanical stirring for 1 h. The GO@CuPc hybrid suspension was then added slowly to the PEN solution in an ultrasonic water bath, and the mixture was stirred by ultrasonic treatment for 30 min at 80°C to produce a homogeneous suspension. Finally, an appropriate amount of the obtained suspension was cast on to a clean glass plate and dried in an oven at 80°C (1 h), 100°C (1 h), 120°C (1 h), 160°C (1 h), and 200°C (1 h), to evaporate the solvent thoroughly. PEN composite films containing different amounts of filler (0, 0.5, 1, 2, 3, 4 and 5 wt.%) were prepared. The thickness of the films (approx. 60 μm) was determined by use of a micrometer caliper.

Characterization

The synthesized products were characterized by use of FTIR spectroscopy (Shimadzu, 8000S), SEM (JSM 6490LV), and TEM (H-600; Hitachi, Japan). The mechanical properties of PEN/GO@CuPc composite films, for example tensile modulus, tensile strength, and elongation at break, were determined by use of a SANS CMT6104 series desktop electromechanical universal testing machine at room temperature. Five different measurements were obtained for each sample and average values were calculated. Differential scanning calorimetry (DSC) was performed with a TA Instruments (New Castle, DE, USA) DSC-Q100 modulated thermal analyzer at a heating rate of 10°/min from room temperature to 350°C. Thermogravimetric analysis (TGA) was performed on TA Instruments TGA-Q50 at a heating rate of 20°/min from room temperature to 800°C. UV–vis absorption spectra were recorded on a UV2501-PC spectrophotometer. Dynamical rheological measurements were obtained by use of a rheometer (TA Instruments AR-G2) with parallel-plate geometry (25 mm diameter). Samples of thickness 1.0 mm and diameter 25 mm were melted at 320°C for 5 min in the parallel-plate fixture to eliminate residual thermal history before measurements were obtained. Dynamic frequency sweep measurements were performed in the angular frequency range of 0.01–100 Hz at 320°C. Dielectric properties were monitored in accordance with ASTM D150 by use of a TH 2819A precision LCR meter.

RESULTS AND DISCUSSION

Characterization of the GO@CuPc Hybrids

The morphology of GO@CuPc hybrids was investigated by SEM and TEM. As shown in Fig. 1a–c, GO sheets were well coated by CuPc nanosized particles, which were deposited densely and evenly

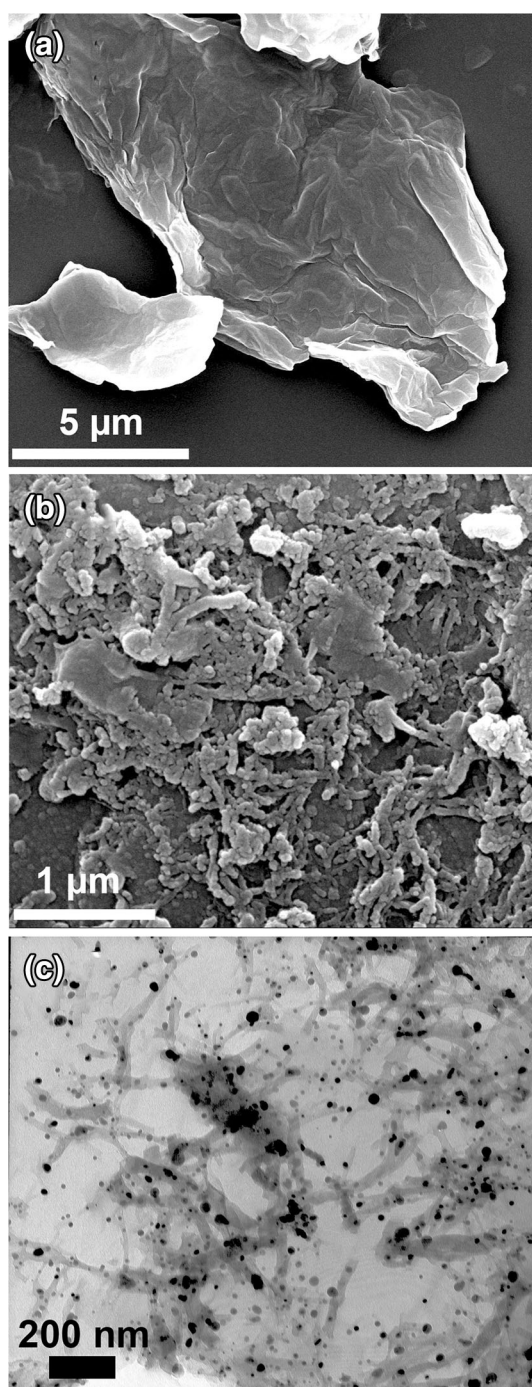


Fig. 1. SEM images of (a) raw GO sheets and (b) GO@CuPc hybrids; TEM image of (c) GO@CuPc hybrids.

on the GO nanosheets to form the fiber-like structure. The fiber-like nanostructure could also be detected on the surface of each GO sheets, indicating that the GO surface had been successfully coated with CuPc by self-assembly.

FTIR was used to confirm the chemical structure of untreated GO and GO@CuPc hybrids; the results are shown in Fig. 2a. The FTIR spectrum of GO

contained a strong, broad absorption band at 3425 cm^{-1} , corresponding to O–H stretching vibration, and a strong peak at approximately 1630 cm^{-1} , attributed to aromatic C=C. An absorption band at 1720 cm^{-1} was attributed to C=O stretching; peaks assigned to carboxy C–O (1402 cm^{-1}), epoxy C–O (1220 cm^{-1}), and alkoxy C–O (1055 cm^{-1}) groups situated at the edges of GO were also observed.¹⁷ After modification by CuPc, absorption bands were observed at 730 cm^{-1} , 1145 cm^{-1} , and 1600 cm^{-1} , corresponding to stretching vibrations of the phthalocyanine ring (Fig. 2a).¹⁸ Absorption bands at 833 cm^{-1} and 1330 cm^{-1} were ascribed to the stretching vibration of NO_2 on the phthalocyanine rings.¹⁸ The sharp characteristic absorption peak of the C=O of –COOH was observed at 1720 cm^{-1} . A clearly observed absorption band at 1470 cm^{-1} was attributed to skeleton vibration of the benzene ring in GO@CuPc. A characteristic aryl ether band at 1230 cm^{-1} was also obtained.¹⁹ The presence of copper phthalocyanine was also confirmed by UV–vis spectroscopy (Fig. 2b). Bands at 630 and 705 nm were characteristic Q-band absorption of GO@CuPc, corresponding to the $\pi\text{--}\pi^*$ transition of the monomer from the HOMO to the LUMO of the Pc^{2-} ring.²⁰

Thermal Properties of PEN/GO@CuPc Composite Films

The thermally induced phase-transition behavior of pure PEN and PEN/GO@CuPc composite films was investigated by DSC under an N_2 atmosphere. The glass transition temperatures (T_g) of the composite films are summarized in Table I. Generally speaking, any structural features that reduce the segmental mobility or free volume will increase T_g . It can be seen from Fig. 3a that the T_g values of the composite films gradually increased with increasing GO@CuPc hybrid content. More importantly, the T_g value of the PEN/GO@CuPc composite film containing 5.0 wt.% GO@CuPc hybrids was 12 degrees higher than that of pure PEN. This is attributed to restriction of molecular movement by the strong binding interaction between GO@CuPc and PEN. The thermal properties of pure PEN and the PEN/GO@CuPc were also determined by TGA in an N_2 atmosphere. TGA curves of the PEN composite films are shown in Fig. 3b. As listed in Table I, all the composite films have high thermal stability with $T_{5\%}$ (initial decomposition temperatures) in the range $470\text{--}483^\circ\text{C}$ and T_{max} (maximum decomposition rate temperature) ranging from 503°C to 510°C . Furthermore, the char yield (C_y) of all the pure PEN and composite films (Table I) are in the range 38–50%. This is mainly attributed to the high thermal stability of the PEN matrix. It can therefore be concluded that the PEN/GO@CuPc composite films have high thermal stability which satisfies the requirements of applications at elevated temperatures and in aggressive chemical environments.

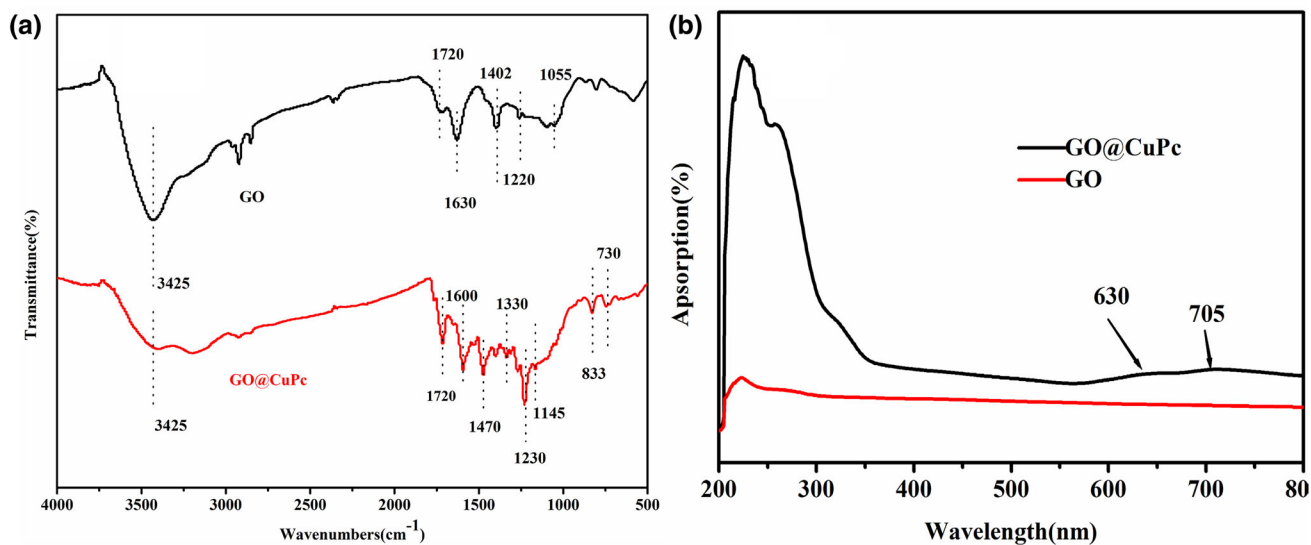


Fig. 2. (a) FTIR spectra of untreated GO and GO@CuPc hybrids; (b) UV-vis spectra of untreated GO and GO@CuPc hybrids.

Table I. Thermal properties of pure PEN and PEN/GO@CuPc composite films

GO@CuPc content (wt.%)	T_g (°C) ^a	$T_{5\%}$ (°C) ^b	T_{max} (°C) ^c	C_y (%) ^d
0	170	475	507	38
0.5	176	470	505	41
1	174	472	503	41
2	175	482	510	40
3	179	483	509	46
4	178	482	509	45
5	182	482	507	50

^aGlass transition temperatures were measured by DSC at a heating rate of 10°/min to 300°C. ^bThe initial decomposition temperatures. ^cMaximum decomposition rate temperature. ^dChar yield at 800°C. All the above were measured in nitrogen.

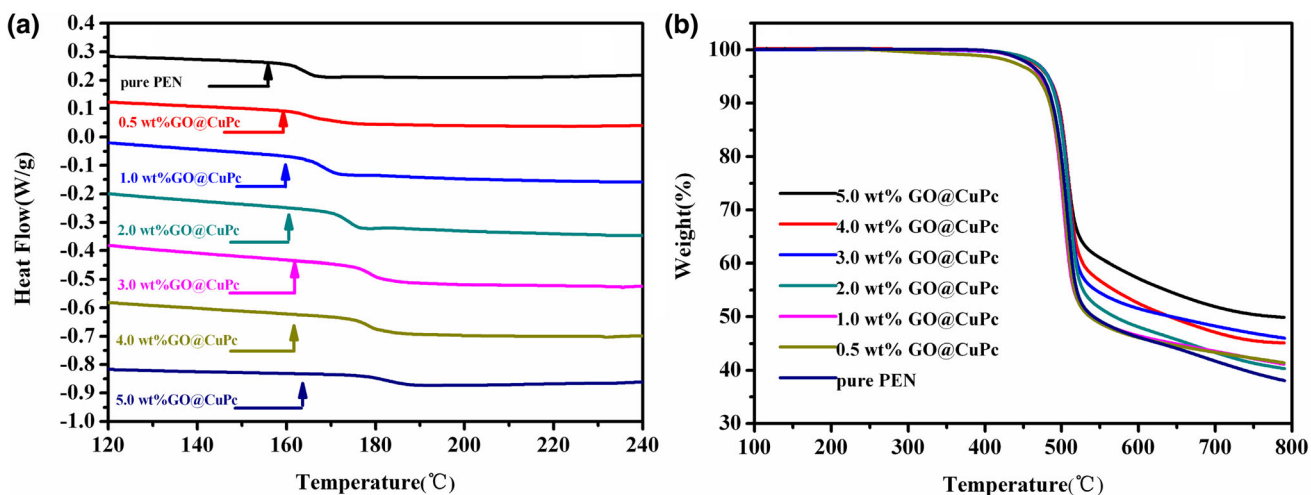


Fig. 3. (a) DSC and (b) TGA curves of pure PEN and PEN/GO@CuPc composite films.

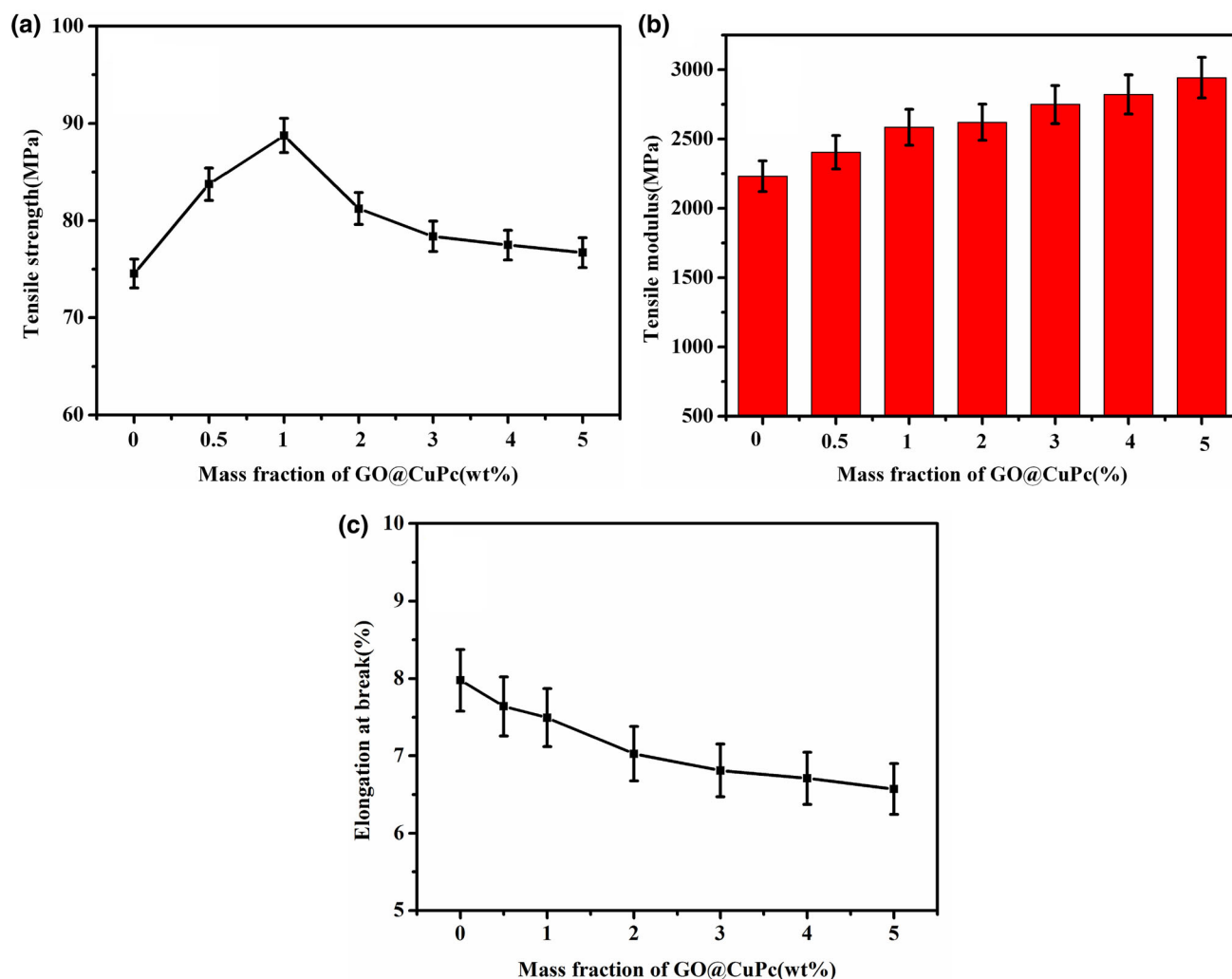


Fig. 4. Mechanical properties of pure PEN and PEN/GO@CuPc composite films: (a) tensile strength; (b) tensile modulus, and (c) elongation at break.

Mechanical Properties of PEN/GO@CuPc Composite Films

Figure 4 shows the mechanical properties of the PEN/GO@CuPc composite films. It is apparent tensile strength reaches its highest value for 1 wt.% GO@CuPc loading (89 MPa) then decreases with further addition of the filler; this may be because of aggregation of GO@CuPc in the polymer matrix as the loading of GO@CuPc is increased. Nonetheless, the tensile modulus of the composite films increased gradually with GO@CuPc hybrid content in the range 0–5 wt.%, as shown in Fig. 4b, which indicates the GO@CuPc hybrids had a greater effect on tensile modulus than on tensile strength. More importantly, the composite films still had excellent flexibility to some extent and a large elongation at break of over 6.6%.

Morphology of PEN/GO@CuPc Composite Films

As reported in the literature, interfacial compatibility between the organic and inorganic phases, and clustering or aggregation of inorganic particles have a large effect on the mechanical properties of composite films.²¹ The mechanical properties of PEN/GO@CuPc composite films could be explained by characterization of the morphology to determine the dispersion of GO@CuPc hybrids in the PEN matrix. As shown in Fig. 5, the surface of pure PEN was smooth and homogeneous (Fig. 5a). However, incorporation of the raw GO sheets and GO@CuPc hybrids significantly changed the surface morphology. For reinforced PEN composite films containing 3.0 wt.% GO@CuPc (Fig. 5b) little aggregation of the hybrids was observed by SEM,

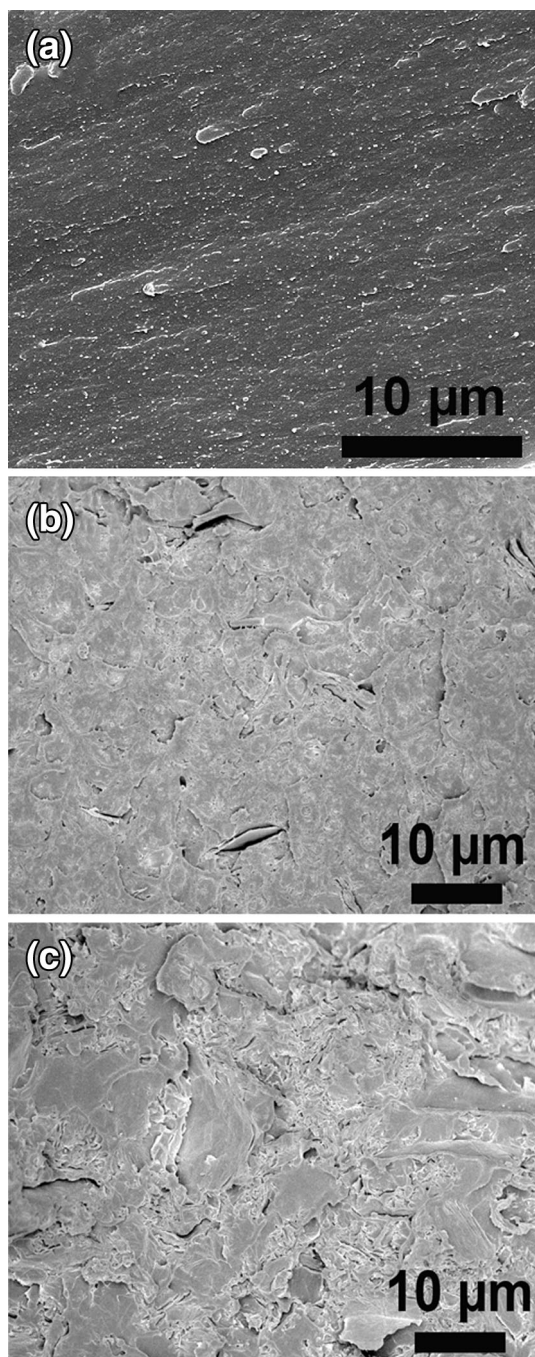


Fig. 5. SEM images of (a) pure PEN, (b) PEN/GO@CuPc nanocomposite film containing 3 wt.% of GO@CuPc hybrids, (c) PEN/GO nanocomposite film containing 3 wt.% of raw GO sheets.

which is indicative good dispersion of the GO@CuPc in the PEN matrix. When loading of the raw GO sheets reaches 3 wt.%, aggregates are clearly apparent (Fig. 5c). These results showed that the interfacial compatibility between raw GO sheets and the PEN matrix had been substantially reduced. By comparison, the GO@CuPc hybrids had better affinity for the PEN matrix. This might be

because the GO@CuPc hybrids and the PEN matrix have abundant strongly polar nitrile groups and similar structures. Therefore, dispersion of the GO@CuPc hybrids in the PEN matrix was better than that of GO in the PEN matrix, which may enhance the properties of PEN/GO@CuPc composite films.

Dielectric Properties of PEN/GO@CuPc Composite Films

Figure 6 shows the dielectric constants and dielectric loss of composite films as frequency was varied at room temperature. The dielectric constants of pure PEN and of PEN/GO@CuPc composite films gradually decrease with increasing frequency in the range 40 Hz to 200 kHz. Variation of the dielectric loss of PEN/GO@CuPc composite films has a similar tendency to that of dielectric constant when the loading content is over 3 wt.%. However, for loadings of 2 wt.% or below the dielectric loss first decreases and then starts to increase slightly at approximately 25 kHz. As shown in Fig. 6a, the dielectric constant and dielectric loss of the composite films (for amounts of GO@CuPc hybrid < 3.0 wt.%) vary slightly and linearly as the frequency increases. This is because the GO@CuPc hybrids did not have enough time to depolarize when the applied frequency was increased. Dielectric loss as the function of frequency is depicted in Fig. 6b. In the alternating electric field, the dielectric loss of the composite films is associated with polarization relaxation and conductivity. As the frequency increased, polarization of GO@CuPc hybrids cannot keep pace with the change of frequency and less energy is consumed, causing the decline of dielectric loss.

The effect of GO@CuPc hybrid content on dielectric constant and dielectric loss of the composite films is depicted in Fig. 7. It is evident that the dielectric constant of the composite films can be enhanced. The dielectric constant of all the films increases linearly with the increasing GO@CuPc hybrid loading; the same behavior is observed for dielectric loss. Obviously, the dielectric constant depends slightly on the change of frequency when the GO@CuPc hybrid loading is below 3.0 wt.%; there is then a turning point at 3.0 wt.%, followed by an abrupt increase in the dielectric constant of the composite films. Similar results are observed for dielectric loss (Fig. 7b). In other words, the percolation threshold of the composite films was approximately 3.0 wt.%. The phenomenon can be explained by the theoretical model of Jonscher.²² As the GO@CuPc loading reached 5.0 wt.%, the dielectric constant reached 52 at 100 Hz. Compared with the dielectric constant of pure PEN, the dielectric constant has increased 14-fold. It is well-recorded that the sharp increment in the dielectric constant of the composites is because of the micro-capacitor effect.²³ In this work, the GO sheets

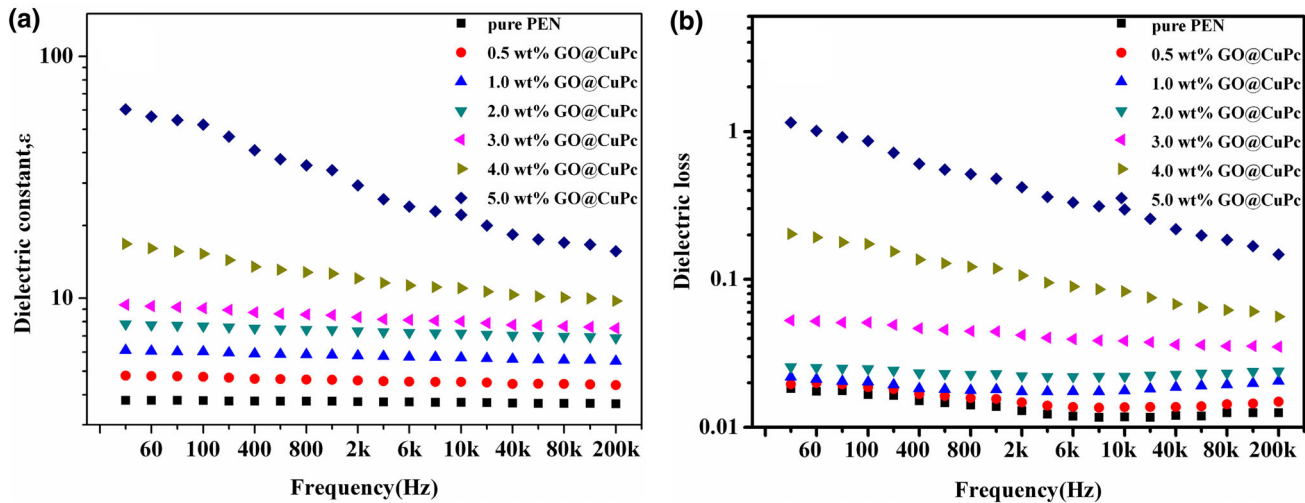


Fig. 6. Effect of frequency on (a) dielectric constant and (b) dielectric loss for pure PEN and for PEN/GO@CuPc composite films.

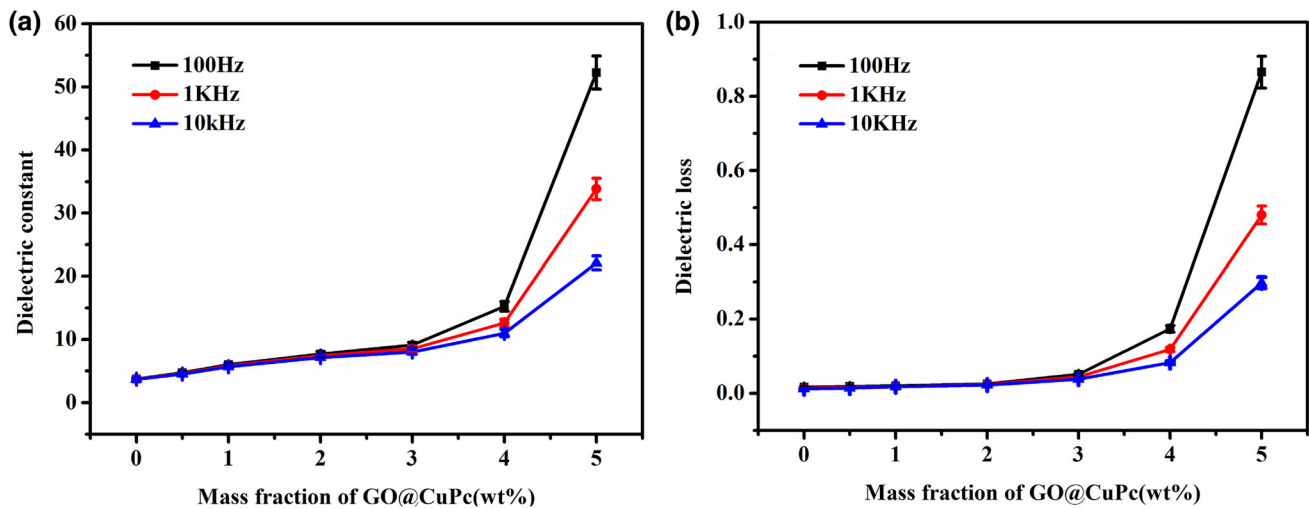


Fig. 7. Effect of GO@CuPc loading on dielectric constant (a) and dielectric loss (b) of pure PEN and PEN/GO@CuPc composite films.

isolated by insulating polymer layers and CuPc particles form many micro-capacitors throughout the composite films; these can cause a substantial increase in the intensity of local electric field and further promote interfacial polarization between the GO sheets and the PEN matrix.

Rheological Properties of PEN/GO@CuPc Composite Films

Rheological measurements were conducted to investigate the effect of GO@CuPc hybrids on the melt-rheological behavior of PEN/GO@CuPc composite films. Figure 8a and b show the storage modulus (G') and loss modulus (G''), respectively, of composite films. It is apparent that the magnitudes of both G' and G'' increase monotonously with increasing frequency for different GO@CuPc content,

especially at low frequency; this is attributed to the reinforcement effect of GO@CuPc. Curves for films with ≤ 2 wt.% loading have similar variation tendency with increasing frequency. However, G' increases substantially at low frequency when the GO@CuPc hybrids content is > 2 wt.%, indicating a sudden change in the inner structure of the composites. This may be mainly attributed to the fact that a network starts to form in the PEN matrix. That is to say, the interactions among hybrids become of primary importance as the filler content increases, eventually leading to a percolation network. This is an indication of transition from liquid-like to solid-like viscoelastic behavior.^{24–28} The tendency for the G'' curves was similar to that for the G' curves. Thus, it is reasonable to assume the GO@CuPc hybrids were well dispersed and

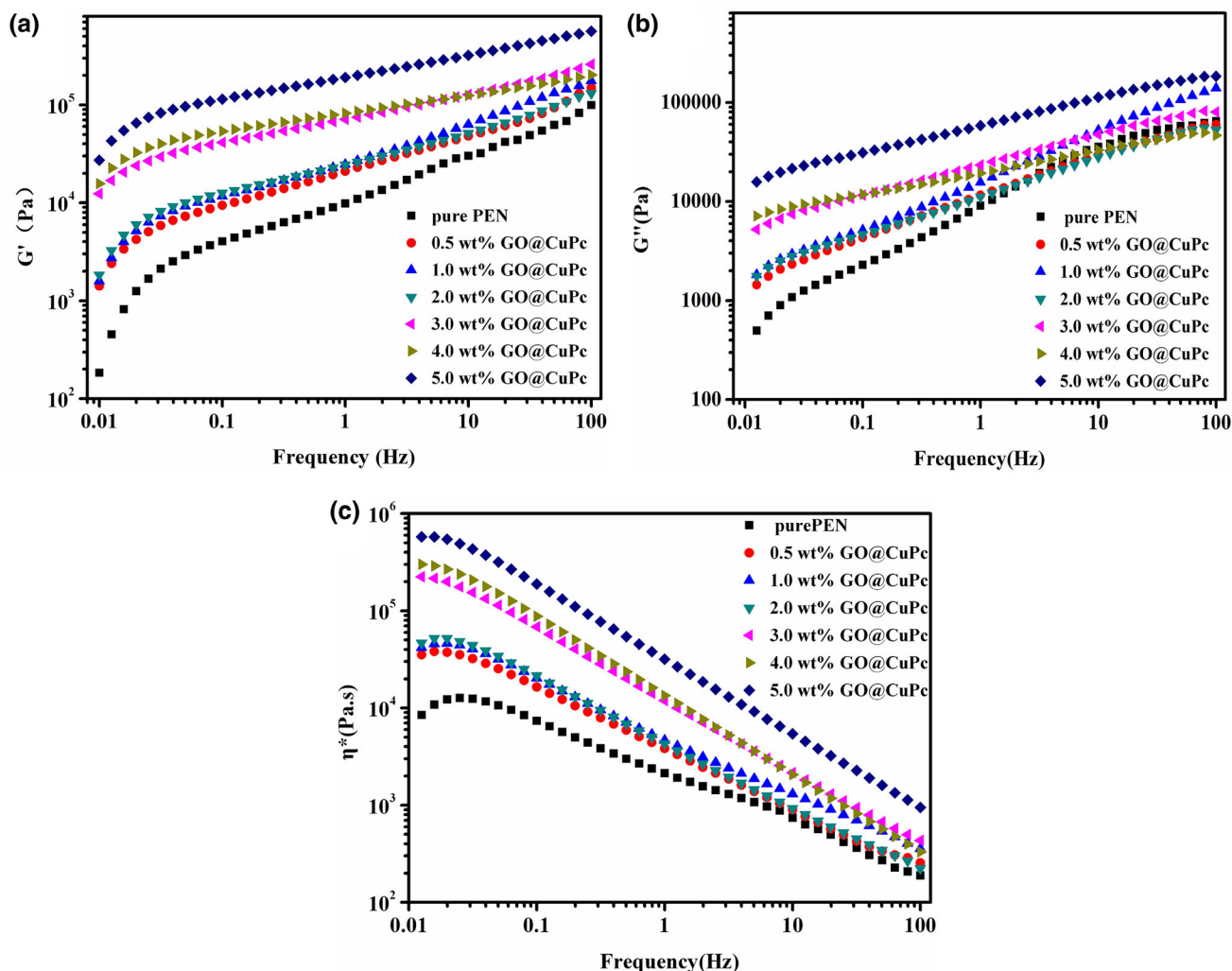


Fig. 8. (a) Storage modulus (G'), (b) loss modulus (G''), and (c) complex viscosity (η^*) of pure PEN and PEN composites with different GO@CuPc loading at 320 °C.

compatible with the PEN matrix, which is also consistent with the SEM results.

Complex viscosity (η^*) is plotted in Fig. 8c. On addition of GO@CuPc hybrid to the PEN matrix the rheological behavior changes, as a result of the change in complex viscosity (η^*). The η^* of PEN indicates PEN is a Newtonian fluid with weak frequency dependence.^{29–33} The η^* of PEN/GO@CuPc composite films is higher than that of pure PEN, and there is a sudden increase for GO@CuPc hybrid contents > 2 wt.%. There is one shear-thinning region, in which η^* decreases linearly with increasing shear rate. Also, because of strong shear-thinning behavior, the GO@CuPc hybrids resulted in a more striking difference of η^* for the composite films at low frequency than at high frequency. As is apparent from Fig. 8c, η^* increased with increasing GO@CuPc hybrid content, demonstrating that the presence of GO@CuPc hybrids caused relaxation of the long PEN polymer chains in the effectively constrained composites. This can be

explained by physical entanglement and chemical interfacial interactions.^{29–33} Therefore, GO@CuPc hybrids were highly compatible with, and were well dispersed in, the PEN matrix.

In addition, it is clear that G' increases rapidly for GO@CuPc hybrids loadings between 2 and 3 wt.% (as shown in Fig. 8a–c), indicating that the films change from the state of solid-like to liquid-like, which is linked with the rheological percolation transition. The storage modulus as a function of the amount of GO@CuPc hybrid at a fixed frequency (0.1 Hz) is depicted in Fig. 9. In this illustration, the sudden change point is the percolation threshold of the composites. The filler changes the local mobility of the polymer chains, only, at low loadings. These restricted areas have a tendency to interact with each other at the percolation threshold, leading to the step change of G' . Thus, the critical factor which decides the change in rheological properties was the state of dispersion.

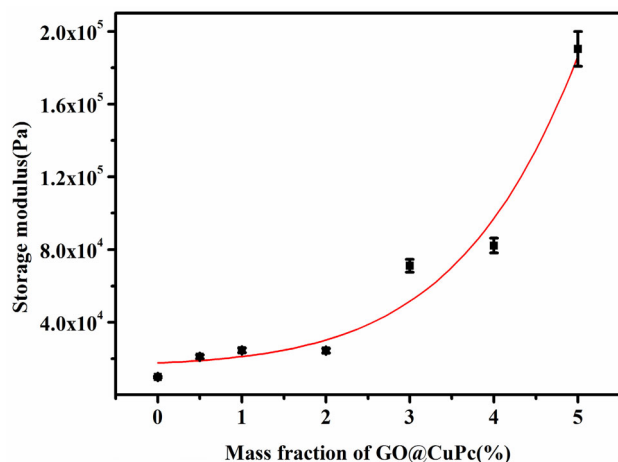


Fig. 9. Plots of dynamic storage modulus (G) at 0.10 Hz as a function of GO@CuPc loading.

CONCLUSIONS

To summarize, PEN/GO@CuPc composites were successfully prepared by a two-step method. The surfaces of GO sheets were coated with the CuPc nanoparticles and the as-prepared hybrid material was then mixed with PEN and films were prepared by solution-casting. DSC and TGA results revealed the composite films had high thermal stability. SEM investigation revealed dispersion of the GO@CuPc hybrids in the PEN matrix was better than that of unmodified GO sheets. Results from mechanical testing showed that the tensile strength was highest when the GO@CuPc loading was 1 wt.%. Furthermore, the dielectric constant of the composite film was as high as 52 at 100 Hz when the GO@CuPc content was 5.0 wt.%. Because of their excellent tensile strength and high dielectric constants, these composite films have enormous potential for use in electric fields, which would benefit from this research.

ACKNOWLEDGEMENTS

The authors wish to thank the National Natural Science Foundation of China (Nos. 51173021, 51373028, 51403029), the "863" National Major Program of High Technology (2012AA03A212), and South Wisdom Valley Innovative Research Team Program (2013B6011) for financial support of this work.

REFERENCES

1. T. Kashiwagi, F. Du, J.F. Douglas, K.I. Winey, R.H. Harris Jr., and J.R. Shields, *Nat. Mater.* 4, 928 (2005).

2. A. Saxena, R. Saxena, V.L. Rao, M. Kanakavel, and K.N. Ninan, *Polym. Bull.* 50, 219 (2003).
3. C. Li, Y. Gu, and X. Liu, *Mater. Lett.* 60, 137 (2005).
4. S. Park and R.S. Ruoff, *Nat. Nanotechnol.* 4, 217 (2009).
5. D.R. Dreyer, R.S. Ruoff, and C.W. Bielawski, *Angew. Chem. Int. Ed.* 49, 9336 (2010).
6. G. Xian, R. Walter, and F. Hauptert, *Compos. Sci. Technol.* 66, 3199 (2006).
7. R.M. Rodgers, H. Mahfuz, V.K. Rangari, N. Chisholm, and S. Jeelani, *Macromol. Mater. Eng.* 290, 43 (2005).
8. H. Wu, C.C. Ma, Y. Yang, H.C. Kuan, C.C. Yang, and C.L. Chiang, *J. Polym. Sci. Pol. Phys.* 44, 1098 (2006).
9. Y. Zhou, P. Farhana, V.K. Rangari, and S. Jeelani, *Mat. Sci. Eng. A* 426, 221 (2006).
10. N. Abacha, M. Kubouchi, K. Tsuda, and T. Sakai, *Express Polym. Lett.* 1, 364 (2007).
11. J. Du, J. Bai, and H. Cheng, *Express. Polym. Lett.* 1, 253 (2007).
12. J. Vickery, A. Patil, and S. Mann, *Adv. Mater.* 21, 2180 (2009).
13. S. Stankovich, R. Piner, S. Nguyen, and R. Ruoff, *Carbon* 44, 3342 (2006).
14. D. Dorina, N. Frank, L. Christiane, M. Martin, and N. Matthias, *Chem. Mater.* 20, 6889 (2008).
15. X. Yang, Y. Lei, J. Zhong, R. Zhao, and X. Liu, *J. Appl. Polym. Sci.* 119, 882 (2011).
16. W.S. Hummers and R.E. Offeman, *J. Am. Chem. Soc.* 80, 1339 (1958).
17. C. Zhu, S. Guo, Y. Fang, and S. Dong, *ACS Nano* 4, 2429 (2010).
18. Z. Guo, C. Shao, M. Zhang, J. Mu, Z. Zhang, P. Zhang, B. Chen, and Y. Liu, *J. Mater. Chem.* 21, 12083 (2011).
19. A. Saxena, V.L. Rao, and K.N. Ninan, *Eur. Polym. J.* 39, 57 (2003).
20. A.W. Snow and N.L. Jarvis, *J. Am. Chem. Soc.* 106, 4706 (1983).
21. J. Zhong, H. Tang, Y. Chen, and X. Liu, *J. Mater. Sci.* 21, 1244 (2010).
22. C. Brosseau, P. Queffelec, and P. Talbot, *J. Appl. Phys.* 89, 4532 (2001).
23. Z. Dang, L. Wang, Y. Yin, and Q. Zhang, *Adv. Mater.* 19, 852 (2007).
24. A.K. Jin, G.S. Dong, J.K. Tae, and R.Y. Jae, *Carbon* 44, 1898 (2006).
25. H.L. Seung, W.K. Myung, H.K. Sung, and R.Y. Jae, *Eur. Polym. J.* 44, 1620 (2008).
26. B. Mathieu, K. Marianna, and E.M. Khalil, *Polymer* 51, 5506 (2010).
27. Q. Zheng, M. Du, B. Yang, and G. Wu, *Polymer* 42, 5743 (2001).
28. D.P.N. Vlasveld, M. Dejong, H.E.N. Bersee, A.D. Gotsis, and S.J. Picken, *Polymer* 46, 10279 (2005).
29. Z. Pu, H. Tang, X. Huang, J. Yang, Y. Zhan, R. Zhao, and X. Liu, *Colloid Surf. A* 415, 125 (2012).
30. A.M. Cynthia, L.B. Jeffrey, A. Sivaram, M.T. James, and K. Ramanan, *Macromolecules* 35, 8825 (2002).
31. P. Potschke, M. Abdel-Goad, I. Alig, S. Dudkin, and D. Lellinger, *Polymer* 45, 8863 (2004).
32. M. Abdalla, D. Dean, D. Adibempe, E. Nyairo, P. Robinson, and G. Thompson, *Polymer* 48, 5662 (2007).
33. R. Kalgaonkar and J. Jog, *Polym. Int.* 57, 114 (2008).